

# Gene delivery to differentiated neurotypic cells with RGD and HIV Tat peptide functionalized polymeric nanoparticles

Jung Soo Suk<sup>a</sup>, Junghae Suh<sup>a</sup>, Kokleong Choy<sup>a</sup>, Samuel K. Lai<sup>b</sup>, Jie Fu<sup>b</sup>, Justin Hanes<sup>a,b,\*</sup>

<sup>a</sup>Department of Biomedical Engineering, The Johns Hopkins University, 3400 N. Charles Street, Baltimore, MD 21218, USA

<sup>b</sup>Department of Chemical & Biomolecular Engineering, The Johns Hopkins University, 3400 N. Charles Street, Baltimore, MD 21218, USA

Received 15 December 2005; accepted 10 May 2006

Available online 12 June 2006

## Abstract

A number of neurodegenerative disorders may potentially be treated by the delivery of therapeutic genes to neurons. Nonviral gene delivery systems, however, typically provide low transfection efficiency in post-mitotic differentiated neurons. To uncover mechanistic reasons for this observation, we compared gene transfer to undifferentiated and differentiated SH-SY5Y cells using polyethylenimine (PEI)/DNA nanocomplexes. Differentiated cells exhibited substantially lower uptake of gene vectors. To overcome this bottleneck, RGD or HIV-1 Tat peptides were attached to PEI/DNA nanocomplexes via poly(ethylene glycol) (PEG) spacer molecules. Both RGD and Tat improved the cellular uptake of gene vectors and enhanced gene transfection efficiency of primary neurons up to 14-fold. RGD functionalization resulted in a statistically significant increase in vector escape from endosomes, suggesting it may improve gene delivery by more than one mechanism.

© 2006 Elsevier Ltd. All rights reserved.

**Keywords:** Gene therapy; CNS diseases; Polymers; Polyethylenimine (PEI)

## 1. Introduction

Gene therapy is a potential strategy to combat neurodegenerative disorders, such as Parkinson's Disease (PD) [1]. For example, successful delivery of genes encoding glial cell line-derived neurotrophic factor (GDNF) [2] and/or tyrosine hydroxylase (TH) (involved in dopamine synthesis) [3] may prevent disease progression and maintain proper dopamine levels despite cell loss caused by PD. GDNF and TH gene delivery using viral vectors, including adenovirus [3,4] and adeno-associated virus [5], provided efficient normalization of function and an increase in survival rate of dopamine-producing neurons in rodents. As an *ex vivo* gene therapy approach, efficient genetic modification of cells was also achieved using recombinant retroviruses [6].

Despite current progress with virus-mediated gene delivery in the CNS, continued development of nonviral vectors is attractive due to the potential for improved safety, reduced immunogenicity, ease of manufacturing and scale up, and the ability to accommodate larger DNA plasmids compared to viral vectors [7,8]. Unfortunately, synthetic systems such as polymer-, lipid- and peptide-based gene carriers are typically much less efficient in delivering genes to primary neurons compared to viral vectors [9]. Thus, identifying bottleneck(s) to efficient nonviral gene delivery in transfection-resistant neurons and testing of new vectors are priorities.

Polyethylenimine (PEI) is currently the most popular polymer used to deliver genes into various cell types [10–13], including neurons [10,11]. PEI is able to condense genes into small nanoparticles [14] and protect the DNA from degradation by nucleases [15]. In addition, the cationic nature of PEI facilitates entry of these gene vectors into cells by binding to negatively charged heparan sulfate proteoglycans on the cell surface [16]. Following internalization, PEI/DNA nanocomplexes are known to efficiently transport toward the perinuclear region of cells

\*Corresponding author. Department of Chemical & Biomolecular Engineering, The Johns Hopkins University, 3400 N. Charles Street, Baltimore, MD 21218, USA. Tel.: +1 410 516 3484; fax: +1 410 516 5510.

E-mail address: [hanes@jhu.edu](mailto:hanes@jhu.edu) (J. Hanes).

[17,18], including primary neurons [19]. PEI is hypothesized to escape endosomes using a proton-sponge effect [20,21], although the mechanism is controversial [22].

In this study, dopaminergic SH-SY5Y neuroblastoma cells were used as an *in vitro* cell model of neurons since they are widely used in PD pathogenesis studies [23,24] and they can be differentiated into neurotypic cells by treatment with retinoic acid (RA) [25]. The mechanism of gene transfer with PEI/DNA nanocomplexes was compared between transfection-permissive undifferentiated [26] and transfection-restrictive differentiated [26,27] SH-SY5Y cells. To improve gene delivery into differentiated neurotypic cells, PEI/DNA nanocomplexes were coated with poly(ethylene glycol) (PEG) after complex formation and bioactive ligands, specifically RGD and HIV-1 Tat peptides, were attached to exposed PEG ends to overcome identified cellular barriers.

## 2. Materials and methods

### 2.1. Cell culture

The SH-SY5Y human neuroblastoma cell line was maintained in a 1:1 mixture of Eagle's minimum essential medium and Ham's F12 nutrient mixture supplemented with 10% fetal bovine serum, penicillin (100 units/ml), streptomycin (100 µg/ml) and 2 mM glutamine. Cells were incubated at 37 °C in a humidified environment with 5% CO<sub>2</sub> atmosphere and passaged every third day with a subcultivation ratio of 1:5.

### 2.2. Cell differentiation

Cells were treated with *all-trans* RA (Sigma, St. Louis, MO) to induce differentiation [25]. RA was added the day after plating at a final concentration of 10 µM in 5% serum media. Differentiation was assessed morphologically by monitoring arrest of cell proliferation and neurite outgrowth at 3 days after RA treatment [25].

### 2.3. Plasmid preparation

Yellow fluorescent protein (YFP)-encoding plasmid (4.7 kbp, as determined by gel electrophoresis) and salmon DNA (2 kbp) were purchased from Clontech (Palo Alto, CA) and Sigma, respectively. Qiagen Maxi Prep kits (Qiagen Inc., Valencia, CA) were used to purify and expand the plasmids, as per manufacturer protocols.

### 2.4. Fluorescent labeling of PEI and complex formulation

PEI (branched, MW = 25 kDa, Sigma) was fluorescently labeled with Oregon Green (OG) 488 (Molecular Probes, Eugene, OR) according to manufacturer's protocol. OG-labeled PEI was purified by size exclusion chromatography using Sephadex G-75 (Sigma) and its concentration was determined by trinitrobenzenesulfonic acid (Sigma) assay [28]. To make PEI/DNA nanocomplexes, PEI was added to 2.5 µg of: (i) YFP-encoding plasmid for transfection assays or (ii) salmon DNA for uptake and colocalization studies (all solutions in 150 mM NaCl with a DNA concentration of 50 µg/ml) at N/P (nitrogen to phosphate) ratio equal to 10, 20 or 30. Amounts of PEI required for gene vectors with different N/P ratios were determined by noting that the molecular weights of a single PEI unit and a single DNA unit are 43.05 and 330.98 g/mole, respectively. The mixture (containing identical volumes of PEI and DNA solutions) was vortexed briefly, and incubated for 30 min at room temperature. Following complex formation, the particle size and zeta potential were

measured using a Zetasizer 3000HS (Malvern Instruments Inc., Southborough, MA).

### 2.5. Surface modification of PEI/DNA nanocomplexes

The four amino acid residue peptide, H-Arg-Gly-Asp-Cys-OH (RGDC) (MW = 451.5 g/mole, Bachem, King of Prussia, PA) and biotin maleimide (MW = 449.49 g/mole, Sigma) were dissolved at 1 mg/ml in 100 mM sodium phosphate buffer (pH 7.0) and dimethylformamide, respectively. To conjugate biotin to the RGDC, solutions were mixed at 1:1 molar ratio and incubated for 3 h at room temperature with occasional stirring. HIV-1 Tat peptide with the sequence YGRKKRRQRRR (MW = 1559.9 g/mole, American Peptide Co., Sunnyvale, CA) was dissolved in 0.5 M sodium phosphate and reacted (1 mg/ml) with high molar excess of citraconic anhydride to reversibly block the primary amine group on the arginine. Biotin hydrazide (MW = 258.34 g/mole, Sigma) was dissolved in dry dimethyl sulfoxide to conjugate to the HIV-1 Tat peptide (0.5 mg/ml). Reaction was completed by incubating for 2 h at room temperature with frequent sonication and dilute HCl was added until a pH of 3 was attained. The product was then dialyzed extensively against PBS using 500/1000 MWCO Float-a-lyzer (Spectrum Lab., Rancho Dominguez, CA) to remove unreacted species.

To attach biotinylated PEG to the surface of PEI/DNA nanocomplexes, biotin-PEG-SPA (MW = 3400 g/mole, NEKTAR, San Carlos, CA) was dissolved in 150 mM NaCl solution (1 mg/ml) and added to the PEI/DNA nanocomplex solution followed by 1 h incubation. The mass ratio of PEG to PEI was 1:9. NeutrAvidin (1 mg/ml in 150 mM NaCl solution, MW = 60 kg/mole, Molecular Probes) was added to PEGylated PEI/DNA nanocomplexes at a molar ratio of 1:1 of NeutrAvidin to biotin-PEG-SPA and, lastly, either biotinylated RGD or HIV-1 Tat protein peptide was added to the complexes. The molar ratio of bioactive ligands (RGD or HIV-1 Tat) to NeutrAvidin was 1:1. It is important to note that RGD has been reported to induce apoptosis by direct caspase-3 activation [29]. However, apoptosis occurred at RGD concentrations of 0.1–1 mM, roughly 1000-fold higher than that used here (0.096 µM).

### 2.6. Determination of ligand conjugation

Following gene vector preparation, the final solution of modified PEI/DNA nanocomplexes was filtered through a Microcon Centrifugal Filter (Millipore, Billerica, MA) to separate unreacted species (i.e., biotinylated peptides) from the particles. The concentration of the unreacted species in the filtrate was determined using the bicinchoninic acid (Pierce, Rockford, IL) protein assay [30]. Less than 5% of free biotinylated peptides were recovered as compared to the starting amount that was added to the complex solution for the surface modification of gene vectors, which suggest that most (>95%) of the peptides are attached to the surface of PEI/DNA nanocomplexes.

### 2.7. Transfection assay

Differentiated and undifferentiated SH-SY5Y cells at 70–80% confluency were transfected with unlabeled PEI/DNA nanocomplexes and incubated for 24 h. Cells were washed twice with PBS, harvested with trypsin/EDTA and washed once again with PBS. Cells were centrifuged at 12,000 rpm for 5 min and the supernatant was discarded. Cells were then resuspended in PBS supplemented with 15 mM EDTA and cell-associated fluorescence was determined using FACScaliber flow cytometer (Becton Dickinson, Franklin Lake, NJ) with a 488 nm excitation laser and a 515 nm emission filter. The concentration of N/P = 20 PEI/DNA complexes used, modified (with RGD or Tat) or unmodified, was always much lower than that where we begin to see significant cytotoxicity (e.g., >95% of cells remained viable upon incubation with each of the complexes studied).

### 2.8. Cellular uptake of labeled nanocomplexes

Fluorescently labeled PEI/DNA nanocomplexes (PEI labeled with OG) of N/P = 20 were added to cells at 70–80% confluency and incubated for 2 h at 4 or 37 °C. Samples at 4 °C served as negative controls since endocytosis does not occur at this lower temperature [31]. The negative control samples were pre-chilled to 4 °C for 30 min prior to addition of nanocomplexes. After 2 h incubation, samples were washed twice with PBS of the corresponding temperature, harvested with trypsin/EDTA and washed once again with PBS. Cells were then centrifuged at 12,000 rpm for 5 min and the supernatant was discarded. Finally, cells were resuspended with PBS supplemented with 15 mM EDTA and cell-associated fluorescence was detected using FACSCaliber flow cytometer (Becton Dickinson) with a 488 nm excitation laser and a 515 nm emission filter.

### 2.9. Co-localization of nanocomplexes and acidic vesicles

Fluorescently labeled PEI/DNA complexes (PEI labeled with OG) carrying 0.5 µg of DNA (N/P ratio = 20 always) were added to differentiated SH-SY5Y cells and incubated at 37 °C for 12 h. LysoTracker Red (Molecular Probes) was added to cells at a final concentration of 100 nM to stain acidic vesicles, specifically late endosomes and lysosomes, 30 min prior to observation. Images of live cells were acquired with confocal microscopy (LSM 510 Meta, Zeiss, Thornwood, NY) with a 100 × /1.4NA oil immersion lens. Cells were maintained at 37 °C during the observation using an air stream stage incubator (Nevtek, Burnsville, VA). Co-localization of complexes and acidic vesicles were quantified by calculating the portion of the overlapping pixels with MetaMorph software (Universal Imaging Co., Downingtown, PA).

## 3. Results

### 3.1. Effect of N/P ratio on gene transfection

We first sought to determine the nitrogen to phosphate ratio (N/P) of PEI/DNA nanocomplexes that led to enhanced transfection of undifferentiated SH-SY5Y cells by measuring YFP expression. PEI/DNA nanocomplexes formulated at N/P = 20 demonstrate approximately 20-fold higher percentage of transfected cells compared to DNA alone (Fig. 1,  $p < 0.01$ , ANOVA). Complexes produced at N/P = 10 and 30 also increase the percentage of transfected cells compared to DNA alone, by 3.4- and 10-fold, respectively ( $p < 0.01$ , ANOVA). In addition,

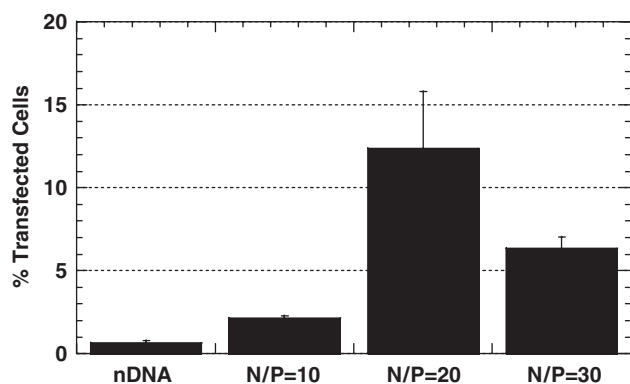


Fig. 1. Percentage of undifferentiated SH-SY5Y cells transfected with DNA alone (nDNA), or PEI/DNA nanocomplexes of N/P = 10, 20 or 30 ( $n = 3$  for each case). Differences in transfection are statistically significant ( $p < 0.01$ , ANOVA).

N/P = 20 complexes yield roughly a 2-fold increase in gene expression per transfected cell (measured as mean YFP fluorescence intensity) compared to DNA alone (data not shown). Although N/P = 30 complexes yield mean fluorescence intensity comparable to N/P = 20 complexes (data not shown), significant cytotoxicity was observed for samples transfected with N/P = 30 complexes. Hence, the N/P = 20 formulation was selected for further study.

### 3.2. Gene delivery to undifferentiated and differentiated neurotypic cells

We sought to uncover bottleneck(s) that may hinder gene delivery to differentiated neurons by comparing the gene delivery process in undifferentiated cells (transfection permissive) to that of differentiated cells (transfection resistant). PEI/DNA nanocomplexes (N/P = 20) carrying plasmid DNA-encoding YFP transfect 4.8-fold fewer differentiated cells than undifferentiated cells (at 24 h post-transfection) and the average YFP gene expression level per transfected cell is about 2-fold lower for differentiated cells (data not shown). Therefore, approximately 10-fold less total YFP is produced by differentiated cells compared to undifferentiated cells.

To begin to understand the mechanistic reasons for the difference in transfection between undifferentiated and differentiated SH-SY5Y cells, we first investigated the role of cellular uptake of gene vectors. Almost 80% of undifferentiated cells internalize PEI/DNA nanocomplexes of N/P = 20, compared to less than 40% of differentiated cells (Fig. 2A). In addition, differentiated cells that contain gene vectors display an approximately 2-fold lower mean fluorescence intensity, corresponding to the amount of gene complexes per cell, compared to undifferentiated cells that contain gene vectors, providing further evidence that endocytosis of gene vectors is significantly hampered in differentiated cells (Fig. 2B and C). Cells incubated at 4 °C exhibit similarly low mean fluorescent intensities for both undifferentiated and differentiated cells, indicating that cellular uptake of gene vectors into both cell types is energy-dependent (Fig. 2B and C). Upon shifting the temperature to 37 °C, both cell types display increased cellular uptake of gene vectors (Fig. 2B).

### 3.3. Gene delivery to differentiated SH-SY5Y cells with modified complexes

To potentially improve the cellular uptake of PEI/DNA nanocomplexes into differentiated neurons, the surfaces of gene vectors were modified with bioactive ligands. First, PEG was covalently coupled to the surface of PEI/DNA nanocomplexes. Upon PEGylation, particle diameter increased slightly, from  $143 \pm 36.1$  to  $156.5 \pm 30.2$  nm, and zeta potential decreased, from  $29.3 \pm 2.3$  to  $22.0 \pm 2.9$  mV. Either RGD or HIV-1 Tat peptides were then attached to the surface of PEI/DNA nanocomplexes via the PEG linkers. Differentiated SH-SY5Y cells were transfected

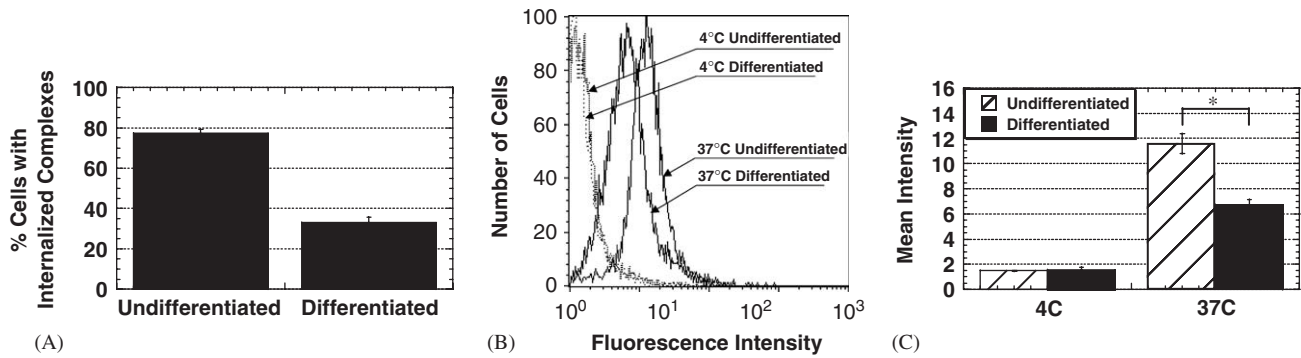


Fig. 2. Cellular uptake of PEI/DNA nanocomplexes (N/P = 20) by undifferentiated and differentiated SH-SY5Y cells at 2 h post-transfection ( $n = 3$  for each case). (A) Percentage of cells with internalized complexes. Difference is statistically significant ( $p < 0.01$ , ANOVA). (B) The distribution of fluorescence intensity of undifferentiated and differentiated SH-SY5Y cells at 4 and 37 °C. (C) Geometric mean fluorescence intensity representing the degree of cellular uptake per cell. Difference in mean fluorescence intensity is statistically significant (\*) for the 37 °C samples ( $p < 0.01$ , ANOVA).

with various complexes: PEI/DNA, PEI/DNA complexes coated with covalently attached PEG grafts (PEI-PEG/DNA) or PEI-PEG/DNA complexes with bioactive ligands attached to their surface at the free end of PEG via biotin-avidin-biotin chemistry (PEI-PEG-RGD/DNA and PEI-PEG-TAT/DNA) (Fig. 3).

Attachment of PEG to PEI/DNA lowered the percentage of transfected differentiated neurons slightly compared to PEI/DNA (approximately 2.5% and 2.1%, respectively; not statistically significant), while attachment of PEG conjugated to either RGD or Tat significantly improved transfection (Fig. 3A). PEI-PEG-RGD/DNA resulted in the greatest improvement in transfection (difference is statistically significant compared to all other complexes, including PEI/DNA controls;  $p < 0.01$ , ANOVA).

Attachment of RGD or Tat also increased gene expression per cell (Fig. 3B). PEI-PEG-RGD/DNA and PEI-PEG-TAT/DNA, enhanced gene expression per cell 4- and 6-fold, respectively, compared to unmodified PEI/DNA. Taking into account increases in the percentage of transfected cells and in gene expression per cell, modified complexes enhance the overall transfection efficiency of differentiated neurotypic cells as much as 14-fold.

### 3.4. Cellular uptake of modified complexes by differentiated neurotypic cells

To determine if enhanced cellular uptake may partially explain the improvement in gene transfection observed with modified complexes, gene vector uptake was quantified by measuring the percentage of cells with internalized complexes and the total amount of cell-associated complexes in studies utilizing PEI that was fluorescently labeled with OG (Fig. 4). Attachment of PEG alone yields a lower percentage of cells with internalized complexes (compared to PEI/DNA) (Figs. 4A and D). However, attachment of RGD or Tat to PEI-PEG/DNA increased overall cellular uptake of gene vectors compared to unmodified PEI/DNA (Fig. 4B and D) and PEI-PEG/DNA (Fig. 4C and D), including the number of gene vectors per cell ( $p < 0.01$ ,

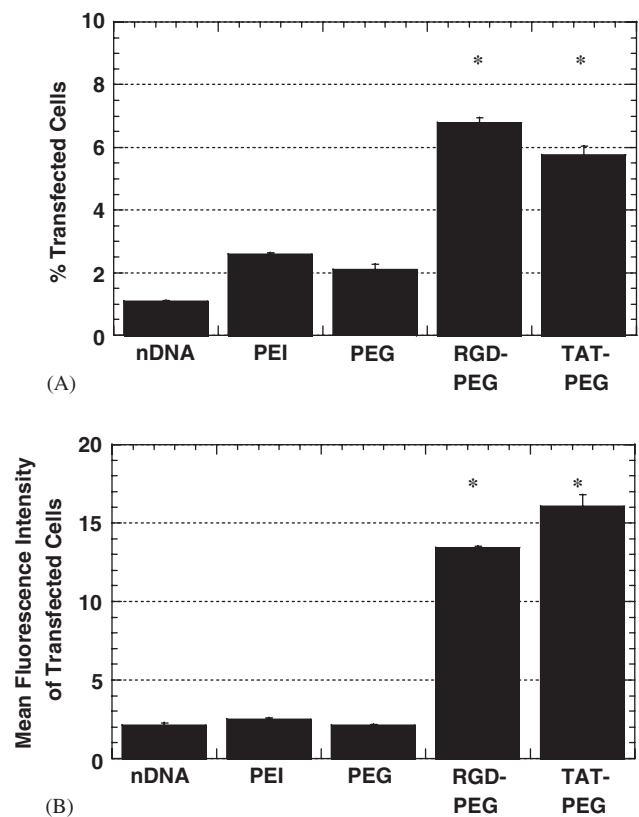


Fig. 3. Transfection efficiency of differentiated SH-SY5Y cells with modified PEI/DNA (PEI) nanocomplexes (N/P = 20) at 24 h post-transfection ( $n = 3$  for each case). Modified complexes include PEI-PEG/DNA (PEG), PEI-PEG-RGD/DNA (RGD-PEG) and PEI-PEG-TAT/DNA (TAT-PEG). Unmodified PEI/DNA nanocomplexes are indicated as PEI. (A) Percentage of transfected cells with various complexes. Differences in percentage of transfected cells is statistically significant compared to PEI/DNA for the samples indicated with an asterisk (\*) ( $p < 0.01$ , ANOVA). (B) Mean fluorescence intensity of transfected cells, represented by YFP gene expression per cell. Difference in mean fluorescence intensity of transfected cells is statistically significant compared to PEI/DNA for the samples indicated with an asterisk (\*) ( $p < 0.01$ , ANOVA).

ANOVA) (Fig. 4E). The mean fluorescence intensity of 4 °C-incubated cells is similar for all complexes, suggesting energy-dependent endocytosis is responsible for cellular

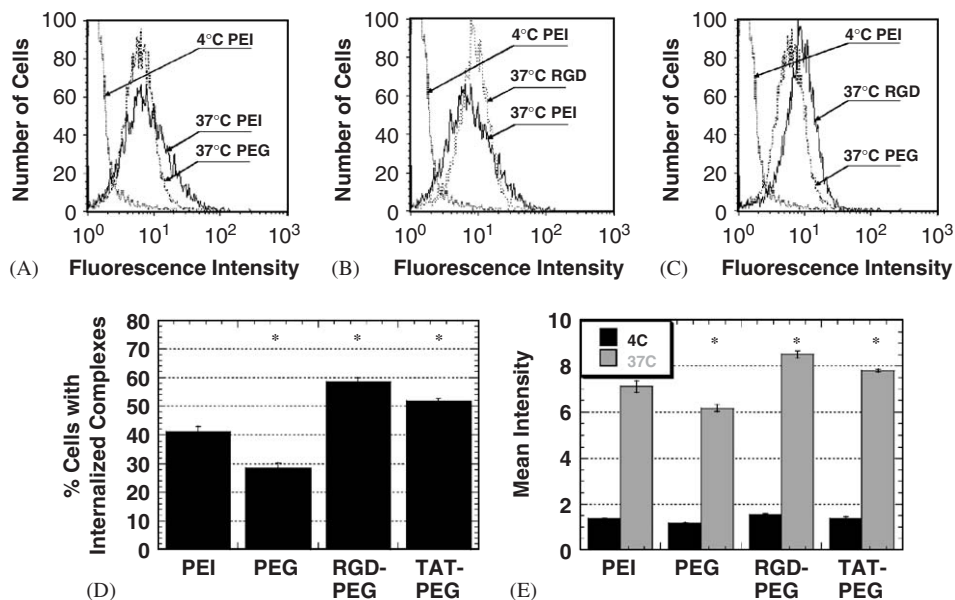


Fig. 4. Cellular uptake of modified PEI/DNA nanocomplexes ( $N/P = 20$ ) at 2 h post-transfection ( $n = 3$  for each case). (A) The distribution of cell-associated fluorescence intensity of cells inoculated with PEI/DNA (4 and 37 °C) and PEI-PEG/DNA (37 °C). (B) The distribution of cell-associated fluorescence intensity of cells inoculated with PEI/DNA (4 and 37 °C) and PEI-PEG-RGD/DNA (37 °C). (C) The distribution of cell-associated fluorescence intensity of PEI/DNA (4 °C), PEI-PEG/DNA (37 °C) and PEI-PEG-RGD/DNA (37 °C). (D) Percentage of cells with internalized complexes at 37 °C. Differences are statistically significant (\*) compared to PEI/DNA ( $p < 0.01$ , ANOVA) (E) Geometric mean fluorescence intensity corresponding to the degree of cellular association at 4 °C (black) and 37 °C (gray). Differences in fluorescence intensity are statistically significant (\*) for all 37 °C samples compared to the 37 °C PEI/DNA sample ( $p < 0.01$ , ANOVA).

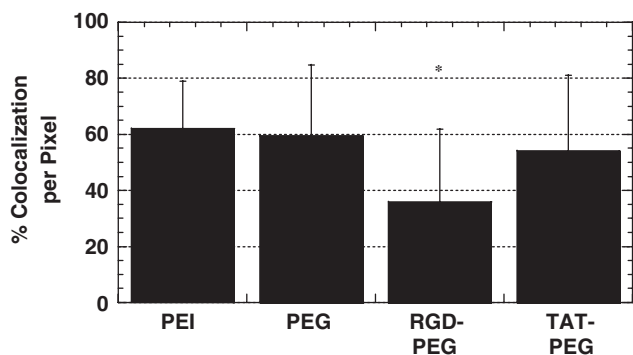


Fig. 5. Percentage of co-localization between PEI/DNA nanocomplexes ( $N/P = 20$ ) and acidic vesicles at 12 h post-transfection, measured by numbers of overlapping pixels ( $n = 50$  cells). PEI-PEG-RGD/DNA (RGD-PEG) displays lowest co-localization, and the difference is statistically significant (\*) ( $p < 0.01$ , ANOVA) compared to all other complexes.

uptake in each case (Fig. 4E). Improved cellular uptake of modified complexes correlated to the enhanced cell transfection (compare Figs. 3A and 4D).

### 3.5. Intracellular trafficking of modified complexes

To determine if the intracellular trafficking of complexes is altered by the addition of bioactive ligands, co-localization studies were performed using a dye that stains acidic vesicles (LysoTracker). Most PEI/DNA nanocomplexes co-localize with lysosomes at 12 h post-transfection (Fig. 5). PEGylation of PEI/DNA nanocomplexes did not

significantly enhance their co-localization with acidic vesicles, as might be expected since PEGylation reduces the amount of free amines available to serve as a proton sponge [20]. Importantly, PEI-PEG-RGD/DNA complexes exhibit statistically significant decrease of co-localization compared to all other complexes (Fig. 5).

## 4. Discussion

Differentiated cells are often relatively resistant to high level of gene transfection with nonviral vectors [32–35], a property observed here with differentiated neurotypic cells. To investigate the mechanistic reason(s) for this result, and in the process begin to uncover the bottlenecks to gene delivery into differentiated neurons, we compared the gene delivery process between differentiated and undifferentiated SH-SY5Y cells. Remarkably, differentiated neurotypic cells endocytosed significantly fewer PEI/DNA nanocomplexes compared to undifferentiated cells, suggesting cell entry of gene vectors may be a critical barrier to efficient gene delivery into differentiated neurons. A similar trend was observed in liposome-mediated gene delivery to differentiated airway epithelial cells [36]. The discrepancy in gene vector uptake may be due to either a difference in density of heparan sulfate on the cell surface or to variations in the structure of heparan sulfate (which is known to be heterogeneous depending on the cell type [37]). Interestingly, Margolis et al. have suggested that nerve growth factor-induced differentiation of PC12 neuroblastoma cells alters the size, charge, and sulfation

pattern of heparan sulfate [38]. These factors may vary the binding affinity/avidity of complexes to the cell surface.

We next sought to improve the cellular uptake of PEI/DNA nanocomplexes into differentiated neurons to see if that would improve overall transfection, as suggested by the large disparity in uptake between undifferentiated and differentiated SH-SY5Y cells. To enhance uptake, we used PEI/DNA nanocomplexes modified with PEG and bioactive ligands specific for cell surface receptors. PEI/DNA nanocomplexes were PEGylated after complex formation in a manner similar to that reported by Ogris et al. [39]. It has been reported that PEGylation of PEI prior to polymer–DNA complexation diminishes the effective targeting and subsequent uptake of bioactive ligand-functionalized gene vectors [40]. However, our modified gene vectors demonstrated improved uptake and gene expression, which may be due to the incorporation of targeting ligands only on the particle surface and not throughout the bulk of the gene vector [39]. Presence of ligands throughout the vector may adversely affect other parameters, such as effective condensation and proper unpacking of cargo DNA. Attachment of ligands via PEG may also be an explanation for the effective cellular uptake of ligand-functionalized gene vectors with high N/P ratios, which is contradictory to previous work done with EGF molecules without PEG spacers [41].

The attachment of RGD or Tat peptides to free PEG ends substantially enhanced overall cellular uptake of gene vectors compared to unmodified vectors. Gene carriers with only NeutrAvidin attached to the PEG linker exhibited cellular uptake similar to PEI–PEG/DNA nanocomplexes (data not shown). Hence, improvement in cellular uptake of modified vectors is not due to nonspecific interaction of NeutrAvidin with the cell surface. This is not surprising since NeutrAvidin has been specifically engineered to minimize nonspecific interactions (that are known to occur with avidin) by making it neutrally charged. As a result of enhanced cellular uptake, both PEI–PEG–RGD/DNA and PEI–PEG–TAT/DNA yield significantly higher transfection efficiencies compared to unmodified PEI/DNA nanocomplexes in differentiated SH-SY5Y cells. The attachment of bioactive ligands to the ends of PEG linkers may enhance the flexibility of the ligands and facilitate the binding of particles to cell surfaces [42]. For example, the use of PEG with conjugated targeting molecules has greatly enhanced drug carrier particle interaction with target cells *in vivo* and under physiologically relevant shear conditions *in vitro* [43].

Efficient internalization of adenovirus into cells is due to the binding of the viral penton base, containing five RGD motifs, to  $\alpha_v\beta_3$  or  $\alpha_v\beta_5$  integrins on the cell surface [44]. RGD binds specifically to nearly half of 20 known integrins on cell surfaces [45] and has been used to improve the cellular uptake of nonviral gene vectors, albeit not in differentiated neurons, by attaching them to liposomes or polymers [46–48]. Binding of adenovirus to the extracel-

lular domain of integrins triggers conformational changes in the integrins [49] and activation of downstream signaling molecules, leading to endocytosis of the virus [50,51]. Thus, attachment of RGD to PEI/DNA nanocomplexes is expected to enhance receptor-mediated endocytosis of the gene vectors in differentiated neurons in a similar manner. The specific binding of RGD motifs to cell surface integrins apparently more than compensates for the decreased nonspecific electrostatic binding upon vector PEGylation.

The HIV-1 Tat peptide exhibits strong binding affinity to cell surface heparan sulfates and induces their aggregation via cross-links [52]. In addition, HIV-1 Tat may bind specifically to glycosaminoglycan-specific structures of heparan sulfate, as suggested for the binding mechanism of viral particles [53]. This property may account for the improved cellular uptake of Tat-modified gene vectors into differentiated neurons. The cell entry mechanism of HIV-1 Tat peptide is controversial in that both energy-dependent endocytosis [54] and energy-independent cell penetration [55] have been suggested. We found that differentiated SH-SY5Y cell entry by Tat-modified gene vectors is energy-dependent.

In both undifferentiated and differentiated cells, PEI/DNA nanocomplexes exhibit similarly high co-localization with late endosomes/lysosomes (LE/Lys) (data not shown), suggesting the sequestration of gene vectors within these vesicles could also be a barrier to efficient transfection. However, since complexes in both differentiated and undifferentiated cells share this property, it seems unlikely that this can explain the difference in transfection efficiency between the two differentiation states. Additionally, intracellular transport of gene vectors to the perinuclear region of neurons may not be a critical obstacle since we recently have shown that PEI/DNA nanocomplexes are actively transported in cells to the perinuclear region along microtubules [17,18], and PEI/DNA nanocomplexes transport in primary neurons at rates similar to those of adenoviruses [19].

Surprisingly, the attachment of RGD ligands, but not Tat ligands, to PEI–PEG/DNA nanocomplexes lowered the co-localization of gene vectors with LE/Lys compared to unmodified PEI/DNA. It is possible that integrin activation by RGD promotes penetration of endosomes by PEI–PEG–RGD/DNA, as suggested for adenoviruses [56].

Finally, it should be noted that the incorporation of PEG to gene vector surfaces may impart several advantageous properties to PEI/DNA nanocomplexes. First, PEI/DNA complexes typically require positive surface charges to bind cell surfaces via nonspecific electrostatic interactions. This property, however, may cause undesired aggregation, opsonization by plasma proteins and systemic toxicity [57] upon *in vivo* administration. PEGylation minimizes these problems by reducing surface charge and by acting as a steric barrier to aggregation [39,57–59]. To this end, it should be noted that we did not add enough PEG to completely shield the surface charge in this work.

Future work should also explore the use of complexes made with a higher PEG to PEI ratio than used here (i.e., higher than 1:9). It should also be mentioned that while Tat is positively charged, it has a significantly lower charge density than unshielded PEI and relatively small amounts may lead to significantly improved carrier uptake and cell transfection, which may allow its use as a ligand in future gene delivery strategies. Indeed, Soundara et al. reported that Tat reduced the cytotoxicity of cationic polyplexes [60]. Even if not, the use of Tat-functionalized gene carriers in this paper serves as positive control related to improved cell uptake and transfection for RGD-functionalized carriers.

## 5. Conclusion

We show that modification of nonviral gene vectors with RGD or Tat peptides via covalently attached PEG chains can enhance gene delivery into differentiated neurons by up to 14-fold *in vitro*. An increase in cellular uptake was observed with RGD- and Tat-modified vectors, and an increase in endosome escape was observed with RGD-modified gene vectors. Further modification of gene vectors to improve their endosome escape and nuclear import may improve gene transfer into differentiated neurons.

## Acknowledgements

The authors thank Drs. Suk Jin Hong and Ted Dawson (Johns Hopkins University, Department of Neuroscience) for helpful discussions. Funding was provided by the NSF (BES 9978160 and 0346716), NIH (T32-GM07057) and an ARCS fellowship to J. Suh.

## References

- [1] Burton EA, Glorioso JC, Fink DJ. Gene therapy progress and prospects: Parkinson's disease. *Gene Ther* 2003;10(20):1721–7.
- [2] Huelbrink CB, Barker RA. The potential of GDNF as a treatment for Parkinson's disease—commentary. *Exp Neurol* 2004;185(1):1–6.
- [3] Corti O, Sanchez-Capelo A, Colin P, Hanoun N, Hamon M, Mallet J. Long-term doxycycline-controlled expression of human tyrosine hydroxylase after direct adenovirus-mediated gene transfer to a rat model of Parkinson's disease. *Proc Natl Acad Sci USA* 1999;96(21):12120–5.
- [4] Chen XW, Liu WG, Yang GY, Liu ZG, Smith S, Calne DB, et al. Protective effects of intracerebral adenoviral-mediated GDNF gene transfer in a rat model of Parkinson's disease. *Parkinsonism Relat Disord* 2003;10(1):1–7.
- [5] Lu YY, Wang LJ, Muramatsu S, Ikeguchi K, Fujimoto K, Okada T, et al. Intramuscular injection of AAV-GDNF results in sustained expression of transgenic GDNF, and its delivery to spinal motoneurons by retrograde transport. *Neurosci Res* 2003;45(1):33–40.
- [6] Horellou P, Mallet J. Gene therapy for Parkinson's disease. *Molec Neurobiol* 1997;15(2):241–56.
- [7] Luo D, Saltzman WM. Synthetic DNA delivery systems. *Nat Biotechnol* 2000;18(1):33–7.
- [8] Pack DW, Hoffman AS, Pun S, Stayton PS. Design and development of polymers for gene delivery. *Nat Rev Drug Discov* 2005;4(7):581–93.
- [9] Berry M, Barrett L, Seymour L, Baird A, Logan A. Gene therapy for central nervous system repair. *Curr Opin Molec Ther* 2001;3(4):338–49.
- [10] Guerra-Crespo M, Charli JL, Rosales-Garcia VH, Pedraza-Alva G, Perez-Martinez L. Polyethylenimine improves the transfection efficiency of primary cultures of post-mitotic rat fetal hypothalamic neurons. *J Neurosci Methods* 2003;127(2):179–92.
- [11] Wu K, Meyers CA, Bennett JA, King MA, Meyer EM, Hughes JA. Polyethylenimine-mediated NGF gene delivery protects transected septal cholinergic neurons. *Brain Res* 2004;1008(2):284–7.
- [12] Gharwan H, Wightman L, Kircheis R, Wagner E, Zatloukal K. Nonviral gene transfer into fetal mouse livers (a comparison between the cationic polymer PEI and naked DNA). *Gene Ther* 2003;10(9):810–7.
- [13] Zaric V, Weltin D, Erbacher P, Remy JS, Behr JP, Stephan D. Effective polyethylenimine-mediated gene transfer into human endothelial cells. *J Gene Med* 2004;6(2):176–84.
- [14] Boussif O, Lezoualch F, Zanta MA, Mergny MD, Scherman D, Demeneix B, et al. A versatile vector for gene and oligonucleotide transfer into cells in culture and *in vivo*: polyethylenimine. *Proc Natl Acad Sci USA* 1995;92(16):7297–301.
- [15] Godbey WT, Barry MA, Saggau P, Wu KK, Mikos AG. Poly(ethylenimine)-mediated transfection: a new paradigm for gene delivery. *J Biomed Mater Res* 2000;51(3):321–8.
- [16] Zou SM, Erbacher P, Remy JS, Behr JP. Systemic linear polyethylenimine (L-PEI)-mediated gene delivery in the mouse. *J Gene Med* 2000;2(2):128–34.
- [17] Suh J, Wirtz D, Hanes J. Real-time intracellular transport of gene nanocarriers studied by multiple particle tracking. *Biotechnol Progr* 2004;20(2):598–602.
- [18] Suh J, Wirtz D, Hanes J. Efficient active transport of gene nanocarriers to the cell nucleus. *Proc Natl Acad Sci USA* 2003;100(7):3878–82.
- [19] Suk JS, Suh J, Lai SK, Hanes J. Quantifying the intracellular transport of viral and nonviral gene vectors in primary neurons. Submitted for publication.
- [20] Behr JP. The proton sponge: a trick to enter cells the viruses did not exploit. *Chimia* 1997;51(1–2):34–6.
- [21] Sonawane ND, Szoka Jr. FC, Verkman AS. Chloride accumulation and swelling in endosomes enhances DNA transfer by polyamine–DNA polyplexes. *J Biol Chem* 2003;278(45):44826–31.
- [22] Forrest ML, Pack DW. On the kinetics of polyplex endocytic trafficking: implications for gene delivery vector design. *Molec Ther* 2002;6(1):57–66.
- [23] Hara H, Ohta M, Ohta K, Kuno S, Adachi T. Increase of antioxidative potential by tert-butylhydroquinone protects against cell death associated with 6-hydroxydopamine-induced oxidative stress in neuroblastoma SH-SY5Y cells. *Molec Brain Res* 2003;119(2):125–31.
- [24] Ben-Shachar D, Zuk R, Gazawi H, Ljubuncic P. Dopamine toxicity involves mitochondrial complex I inhibition: implications to dopamine-related neuropsychiatric disorders. *Biochem Pharmacol* 2004;67(10):1965–74.
- [25] Simpson PB, Bacha JL, Palfreyman EL, Woollacott AJ, McKernan RM, Kerby J. Retinoic acid-evoked differentiation of neuroblastoma cells predominates over growth factor stimulation: an automated image capture and quantitation approach to neuritogenesis. *Anal Biochem* 2001;298(2):163–9.
- [26] Almeida A, Bolanos JP, Moreno S. Cdh1/Hct1-APC is essential for the survival of postmitotic neurons. *J Neurosci* 2005;25(36):8115–21.
- [27] Liu G, Li D, Pasumarthy MK, Kowalczyk TH, Gedeon CR, Hyatt SL, et al. Nanoparticles of compacted DNA transfect postmitotic cells. *J Biol Chem* 2003;278(35):32578–86.
- [28] Snyder SL, Sobocinski PZ. Improved 2,4,6-trinitrobenzenesulfonic acid method for determination of amines. *Anal Biochem* 1975;64(1):284–8.

- [29] Buckley CD, Pilling D, Henriquez NV, Parsonage G, Threlfall K, Scheel-Toellner D, et al. RGD peptides induce apoptosis by direct caspase-3 activation. *Nature* 1999;397(6719):534–9.
- [30] Tyllianakis PE, Kakabakos SE, Evangelatos GP, Ithakissios DS. Direct colorimetric determination of solid-supported functional groups and ligands using bicinchoninic acid. *Anal Biochem* 1994;219(2):335–40.
- [31] Watson P, Jones AT, Stephens DJ. Intracellular trafficking pathways and drug delivery: fluorescence imaging of living and fixed cells. *Adv Drug Deliv Rev* 2005;57(1):43–61.
- [32] Florea BI, Meaney C, Junginger HE, Borchard G. Transfection efficiency and toxicity of polyethylenimine in differentiated Calu-3 and nondifferentiated COS-1 cell cultures. *AAPS Pharmsci* 2002;4(3):E12.
- [33] Abdallah B, Hassan A, Benoist C, Goula D, Behr JP, Demeneix BA. A powerful nonviral vector for *in vivo* gene transfer into the adult mammalian brain: polyethylenimine. *Hum Gene Ther* 1996;7(16):1947–54.
- [34] Horbinski C, Stachowiak MK, Higgins D, Finnegan SG. Polyethylenimine-mediated transfection of cultured postmitotic neurons from rat sympathetic ganglia and adult human retina. *BMC Neurosci* 2001;2(1):2.
- [35] Cryan SA, O'Driscoll CM. Mechanistic studies on nonviral gene delivery to the intestine using *in vitro* differentiated cell culture models and an *in vivo* rat intestinal loop. *Pharm Res* 2003;20(4):569–75.
- [36] Matsui H, Johnson LG, Randell SH, Boucher RC. Loss of binding and entry of liposome–DNA complexes decreases transfection efficiency in differentiated airway epithelial cells. *J Biol Chem* 1997;272(2):1117–26.
- [37] Medeiros GF, Mendes A, Castro RAB, Bau EC, Nader HB, Dietrich CP. Distribution of sulfated glycosaminoglycans in the animal kingdom: widespread occurrence of heparin-like compounds in invertebrates. *Biochim Biophys Acta—Gen Subjects* 2000;1475(3):287–94.
- [38] Margolis RK, Salton SR, Margolis RU. Effects of nerve growth factor-induced differentiation on the heparan sulfate of PC12 pheochromocytoma cells and comparison with developing brain. *Arch Biochem Biophys* 1987;257(1):107–14.
- [39] Ogris M, Walker G, Blessing T, Kircheis R, Wolschek M, Wagner E. Tumor-targeted gene therapy: strategies for the preparation of ligand–polyethylene glycol–polyethylenimine/DNA complexes. *J Control Rel* 2003;91(1–2):173–81.
- [40] Kunath K, Merdan T, Hegener O, Haberlein H, Kissel T. Integrin targeting using RGD-PEI conjugates for *in vitro* gene transfer. *J Gene Med* 2003;5(7):588–99.
- [41] Schaffer DV, Lauffenburger DA. Optimization of cell surface binding enhances efficiency and specificity of molecular conjugate gene delivery. *J Biol Chem* 1998;273(43):28004–9.
- [42] Kursu M, Walker GF, Roessler V, Ogris M, Roedel W, Kircheis R, et al. Novel shielded transferrin-polyethylene glycol-polyethylenimine/DNA complexes for systemic tumor-targeted gene transfer. *Bioconjugate Chem* 2003;14(1):222–31.
- [43] Sakhalkar HS, Dalal MK, Salem AK, Ansari R, Fu A, Kiani MF, et al. Leukocyte-inspired biodegradable particles that selectively and avidly adhere to inflamed endothelium *in vitro* and *in vivo*. *Proc Natl Acad Sci USA* 2003;100(26):15895–900.
- [44] Medina-Kauwe LK. Endocytosis of adenovirus and adenovirus capsid proteins. *Adv Drug Deliv Rev* 2003;55(11):1485–96.
- [45] Ruoslahti E. RGD and other recognition sequences for integrins. *Annu Rev Cell Dev Biol* 1996;12:697–715.
- [46] Harvie P, Dutzar B, Galbraith T, Cudmore S, O'Mahony D, Anklesaria P, et al. Targeting of lipid–protamine–DNA (LPD) lipopolyplexes using RGD motifs. *J Liposome Res* 2003;13(3–4):231–47.
- [47] Wittekindt C, Bottger M, Holtje HD, Schafer-Korting M, Cartier R, Haberland A. Integrin-specificity of the cyclic Arg-Gly Asp motif and its role in integrin targeted gene transfer. *Biotechnol Appl Biochem* 2004.
- [48] Colin M, Harbottle RP, Knight A, Kornprobst M, Cooper RG, Miller AD, et al. Liposomes enhance delivery and expression of an RGD-oligolysine gene transfer vector in human tracheal cells. *Gene Ther* 1998;5(11):1488–98.
- [49] Arnaout MA, Goodman SL, Xiong JP. Coming to grips with integrin binding to ligands. *Curr Opin Cell Biol* 2002;14(5):641–51.
- [50] Wickham TJ, Mathias P, Cheres DA, Nemerow GR. Integrin- $\alpha$ -V- $\beta$ -3 and integrin- $\alpha$ -V- $\beta$ -5 promote adenovirus internalization but not virus attachment. *Cell* 1993;73(2):309–19.
- [51] Li E, Stupack D, Klemke R, Cheres DA, Nemerow GR. Adenovirus endocytosis via  $\alpha$ (v) integrins requires phosphoinositide-3-OH kinase. *J Virol* 1998;72(3):2055–61.
- [52] Ziegler A, Seelig J. Interaction of the protein transduction domain of HIV-1 TAT with heparan sulfate: binding mechanism and thermodynamic parameters. *Biophys J* 2004;86(1):254–63.
- [53] Tamura M, Natori K, Kobayashi M, Miyamura T, Takeda N. Genogroup II noroviruses efficiently bind to heparan sulfate proteoglycan associated with the cellular membrane. *J Virol* 2004;78(8):3817–26.
- [54] Vives E. Cellular uptake of the Tat peptide: an endocytosis mechanism following ionic interactions. *J Molec Recogn* 2003;16(5):265–71.
- [55] Jarver P, Langel U. The use of cell-penetrating peptides as a tool for gene regulation. *Drug Discov Today* 2004;9(9):395–402.
- [56] Wang K, Guan TL, Cheres DA, Nemerow GR. Regulation of adenovirus membrane penetration by the cytoplasmic tail of integrin  $\beta$  5. *J Virol* 2000;74(6):2731–9.
- [57] Ogris M, Brunner S, Schuller S, Kircheis R, Wagner E. PEGylated DNA/transferrin-PEI complexes: reduced interaction with blood components, extended circulation in blood and potential for systemic gene delivery. *Gene Ther* 1999;6(4):595–605.
- [58] Fu J, Fiegel J, Krauland E, Hanes J. New polymeric carriers for controlled drug delivery following inhalation or injection. *Biomaterials* 2002;23(22):4425–33.
- [59] Fiegel J, Fu J, Hanes J. Poly(ether-anhydride) dry powder aerosols for sustained drug delivery in the lungs. *J Control Rel* 2004;96(3):411–23.
- [60] Soundara Manickam D, Bisht HS, Wan L, Mao G, Oupicky D. Influence of TAT-peptide polymerization on properties and transfection activity of TAT/DNA polyplexes. *J Control Rel* 2005;102(1):293–306.